

Physical Principles of Circular Dichroism

Steven S. Andrews* and James Tretton



Cite This: *J. Chem. Educ.* 2020, 97, 4370–4376



Read Online

ACCESS |

Metrics & More

Article Recommendations

ABSTRACT: Circular dichroism (CD) is the differential absorption of left and right circularly polarized light. It arises from molecular electron oscillations that are driven by both the light's electric and magnetic fields, where the effects are in phase for one circular polarization and out of phase for the other. We describe these interactions, which have not been presented at an intuitive level before, with classical and quantum treatments. A rotational average of the latter solution leads to the Rosenfeld equation, which underlies most CD research. We illustrate its use with a chiral version of a harmonic oscillator, which we then apply to the far-ultraviolet CD of protein α -helices. This presentation is aimed at the level of upper-division undergraduates and could be usefully incorporated into a physical chemistry course.

KEYWORDS: *Upper-Division Undergraduate, Biochemistry, Physical Chemistry, Analogies/Transfer, Biophysical Chemistry, Chirality/Optical Activity, Proteins/Peptides, Quantum Chemistry, Spectroscopy, Theoretical Chemistry*

INTRODUCTION

Circular dichroism (CD) is a spectroscopy technique that measures the absorption difference between left and right circularly polarized light. By symmetry, this asymmetric absorption can only occur for asymmetric molecules, meaning chiral molecules. Ultraviolet CD has found a particular application for empirically assessing protein secondary structure, enabling a quick determination of whether a protein is primarily α -helix, β -sheet, or unfolded.^{1–3} Vibrational CD, in the infrared, is especially useful for determining the structures of small molecules.^{4–6} CD has also been explored theoretically for over a century,^{7–9} culminating in a thorough understanding that is sufficient for accurately predicting many CD spectra from molecular structures, although these calculations typically require substantial computation. However, the physical principles that produce CD do not appear to have been described previously at an intuitive level, which is the focus of the current work.

Superficially, it seems obvious that chiral molecules would absorb left and right circularly polarized light slightly differently, creating CD effects, but more careful thought shows that it is not so simple. The problem is that most molecules are much smaller than a light wavelength, so it is physically impossible for a molecule, regardless of its chirality, to respond differently to spatial aspects of light waves, including whether the wave shape is right- or left-handed. Instead, all that a molecule is “aware of” are the electromagnetic fields at the molecule's location, which are essentially the same for left and right circularly polarized light, especially when considering effects on unoriented samples. The answer is that CD effects arise from molecular interactions with *both* the light's electric and magnetic fields, forming an unusual type of interaction between light and matter.

Here, we explain the physical principles of CD for upper-level undergraduate students. We present a classical treatment,

which appears to be new, and a more conventional quantum treatment that builds on prior work.^{10–12} We illustrate the quantum results with a simple harmonic oscillator model, which we then use to estimate the CD peak area for a protein α -helix. The result is only about a factor of 4 larger than experimental results, which is remarkably close for such a complex system.

THEORY

Light Polarization

We focus on a plane wave that is propagating toward the positive x -axis, so its electric field (E -field) varies as¹³

$$\tilde{\mathbf{E}}(t) = E_0 \hat{\mathbf{e}} e^{i(kx - \omega t)} \quad (1)$$

The tilde indicates a complex value, of which only the real portion is physically meaningful. On the right side, E_0 is the wave amplitude, $\hat{\mathbf{e}}$ is a polarization vector with unit magnitude, and the exponential expresses the wave's oscillation, where κ is the spatial frequency and ω is the temporal frequency (both measured in radians). The polarization vector equals $\hat{\mathbf{z}}$ (unit vector on z -axis) for vertically polarized light, $\hat{\mathbf{y}}$ for horizontally polarized light, $\hat{\mathbf{r}}$ for right circularly polarized light (RCP), and $\hat{\mathbf{l}}$ for left circularly polarized light (LCP), as observed when facing the source (Figure 1A,B). These latter unit vectors are

Received: August 8, 2020

Revised: October 25, 2020

Published: November 16, 2020



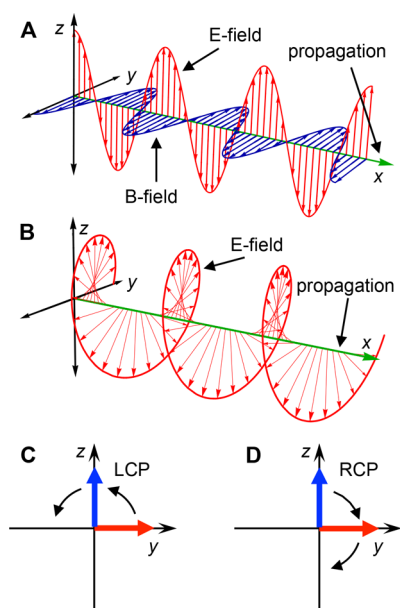


Figure 1. Light polarization, shown with the E-field in red and B-field in blue. (A) Vertically polarized light with polarization vector $\hat{\mathbf{e}} = \hat{\mathbf{z}}$. (B) E-field of right circularly polarized light (RCP) with the B-field not shown for clarity, $\hat{\mathbf{e}} = \hat{\mathbf{r}}$. (C) Fields at the origin for LCP, facing backward along the propagation direction, $\hat{\mathbf{e}} = \hat{\mathbf{I}}$. (D) Fields at the origin for RCP, $\hat{\mathbf{e}} = \hat{\mathbf{r}}$.

$$\hat{\mathbf{r}} = \frac{1}{\sqrt{2}} \begin{bmatrix} 0 \\ 1 \\ -i \end{bmatrix} = \frac{\hat{\mathbf{y}} - i\hat{\mathbf{z}}}{\sqrt{2}} \quad (2)$$

$$\hat{\mathbf{I}} = \frac{1}{\sqrt{2}} \begin{bmatrix} 0 \\ 1 \\ i \end{bmatrix} = \frac{\hat{\mathbf{y}} + i\hat{\mathbf{z}}}{\sqrt{2}} \quad (3)$$

For circularly polarized light, the magnetic field (B-field) rotates over time and space in the same direction as the E-field but is a quarter cycle out of phase, leading for LCP and lagging for RCP (Figure 1C,D). Combining this phase shift with the fact that the B-field amplitude¹³ is equal to E_0/c , where c is the speed of light, gives the complex B-field for circularly polarized light as

$$\tilde{\mathbf{B}}(t) = \pm \frac{i}{c} \tilde{\mathbf{E}}(t) \quad (4)$$

Here, and below, the upper sign is for RCP, and the lower is for LCP.

Induced Static Dipole Moment

We choose an electrically conducting helix as a model chiral molecule. Supposing its axis is parallel to the light propagation direction (Figure 2), the rotating electric field of circularly polarized light would, presumably, push electric charge around the helix, winding the charge toward one of the helix ends rather like water being transported with an Archimedes screw. This would create a static dipole moment in the molecule that is aligned with the light propagation direction. Although it has not been reported before, to our knowledge, this would presumably change the molecule's absorption spectrum, either from the charge rearrangement altering the molecular energy levels or from the electric field of the induced dipole moment modifying the absorption spectrum through Stark effects.^{14,15}

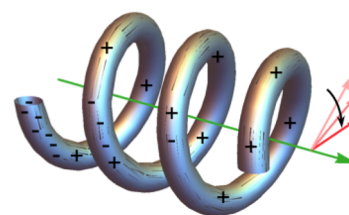


Figure 2. Helical molecule oriented parallel to the propagation direction of RCP light (green arrow). Red arrows show the light's E-field. Positive charges are immobile while negative charges get wound to a helix end.

However, this induced dipole moment would not produce CD for unoriented samples because molecules with one orientation in RCP light would have the same absorption as

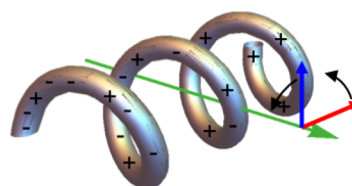


Figure 3. Helix oriented perpendicular to the propagation direction of LCP light, shown with the green arrow. Red and blue arrows show the light's E- and B-fields, respectively. Positive charges are immobile while negative charges get pushed toward the left side of the helix, at this particular moment, due to the directions of both the light's E-field and changing B-field.

molecules with the opposite orientation in LCP light. Thus, any CD effects would cancel out. On the other hand, this analysis makes the intriguing prediction that absorption spectra would differ between circularly polarized light, where a dipole moment is induced, and linearly polarized light, where one is not.

Classical Explanation for CD

Next, suppose the helix axis is parallel to the z -axis (Figure 3). Now, the z -component of the light wave's E-field pushes electric charge back and forth along the length of the helix. Meanwhile, the temporal change in the z -component of the light wave's B-field induces a current around the helix, which also drives electric charge back and forth along the length of the helix. These two effects are in phase for one circular polarization and out of phase for the other, causing different amounts of electric current in the helix. As a result, the two circular polarizations are absorbed to different extents, which creates the CD effects that are normally observed.¹⁶ The following analysis quantifies these effects.

The helical molecule shape can be expressed mathematically as

$$\begin{aligned} x &= r \cos \chi \\ y &= r \sin \chi \\ z &= d\chi \end{aligned} \quad (5)$$

where r is the radius, χ is the azimuthal angle, meaning the angle measured around the z -axis, and d is the helix pitch rate, meaning the distance that the helix advances along the z -axis as it goes through one radian of angle (Figure 4). Additionally, we define the position along the helix path as s , which ranges from

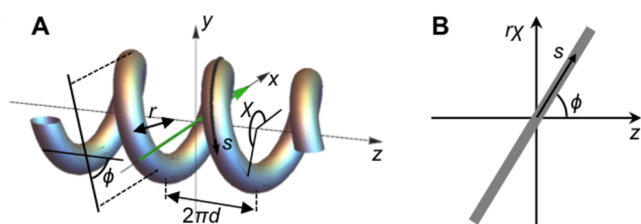


Figure 4. Parameters for a right-handed helix. (A) Three-dimensional picture. (B) Unrolled helix, shown with the gray line, in which the helix axis is along z and the circumference is unrolled vertically, along $r\chi$. ϕ is the helix pitch angle.

a negative value at one helix end to a positive value at the opposite end, and the pitch angle as ϕ , which represents the slope of the helix when viewed from the side; ϕ is zero for a helix that is stretched out to a straight rod, $\pm\pi/2$ for one that is compressed into a circle, positive for a right-handed helix, and negative for a left-handed helix. Unrolling the helix shows that $z = s \cos \phi$ and $r\chi = s \sin \phi$.

From eqs 1, 2, and 3, the z -component of the \mathbf{E} -field of circularly polarized light varies over time at the origin as $\mp E_0 \sin(\omega t) / \sqrt{2}$. The electromotive force that drives the electrons along the helical wire is the component of this field that is parallel to the path of the helix, introducing a factor of $\cos \phi$ to the field. Thus, the component of the light's \mathbf{E} -field along the helix path is

$$E_E(t) = \mp \frac{E_0}{\sqrt{2}} \sin(\omega t) \cos \phi \quad (6)$$

This result is averaged over many helix turns to account for the fact that the y -component of the light's rotating \mathbf{E} -field also contributes some to the \mathbf{E} -field along the helix path, but these contributions average to zero over many turns.

A consequence of Faraday's law is that a changing \mathbf{B} -field induces an electric field in a circular wire that is perpendicular to the field, with strength¹³ $E = -r\dot{B}/2$. The electromotive force along the path of the helical wire is proportional to the component of the \mathbf{B} -field that is perpendicular to the path, so the induced electric field is

$$E_B(t) = -\frac{r}{2} \dot{B}_z(t) \sin \phi \quad (7)$$

Again, this represents an average over many helix turns. Taking the z -component of the \mathbf{B} -field from eq 4, differentiating over time, and substituting the result into eq 7 gives

$$E_B(t) = \frac{r\omega E_0}{2c\sqrt{2}} \sin(\omega t) \sin \phi \quad (8)$$

The total electric field along the helix path is the sum of these contributions

$$\begin{aligned} E_{\text{total}}(t) &= E_E(t) + E_B(t) \\ &= \frac{E_0}{\sqrt{2}} \sin(\omega t) \left(\mp \cos \phi + \frac{r\omega}{2c} \sin \phi \right) \end{aligned} \quad (9)$$

Assume the electric current in the helix can be found from Ohm's law, which can be given as $I(t) = \sigma a E_{\text{total}}(t)$, where $I(t)$ is the current, σ is the electrical conductivity of the helical wire, and a is the cross-sectional area of this wire.¹³ This assumption is severe, as discussed below, but still useful. Combining this with eq 9 gives the current in the helix

$$I(t) = \frac{\sigma a E_0}{\sqrt{2}} \sin(\omega t) \left(\mp \cos \phi + \frac{r\omega}{2c} \sin \phi \right) \quad (10)$$

The power dissipated by the helix is given by $P = IV$, where I is the current and V is the voltage over the total helix path length, L . The voltage is the electric field along the path times the length of the path, so the dissipated power is

$$P(t) = \frac{\sigma a L r \omega E_0^2}{2} \sin^2(\omega t) \left(\cos^2 \phi + \frac{r^2 \omega^2}{4c^2} \sin^2 \phi \mp \frac{r\omega}{c} \cos \phi \sin \phi \right) \quad (11)$$

The first term in parentheses represents light absorption by the \mathbf{E} -field alone and is largest when $\phi = 0$, meaning that the helix is stretched out to a straight rod; the second term represents light absorption by the \mathbf{B} -field alone and is largest when $\phi = \pm\pi/2$, meaning that the helix is compressed to a circle, and the final term shows different absorption amounts for the two circular polarizations, producing CD.

Defining the CD signal as the difference between LCP and RCP absorption, as is typical, the CD dissipated power is

$$P_{\text{CD}}(t) = \frac{\sigma a L r \omega E_0^2}{c} \sin^2(\omega t) \cos \phi \sin \phi \quad (12)$$

Averaging over many light cycles replaces the $\sin^2(\omega t)$ term with its average of $1/2$, giving

$$P_{\text{CD}} = \frac{\sigma a L r \omega E_0^2}{2c} \cos \phi \sin \phi \quad (13)$$

Thus, the CD signal is proportional to the helix conductivity, the helix wire cross-sectional area, and the total helix path length, all of which are intuitively reasonable. It is also proportional to r and ω , from the \mathbf{B} -field influence. The proportionality to the square of the applied \mathbf{E} -field is consistent with wave power being proportional to the squared amplitude. Finally, the CD signal is proportional to $\cos \phi \sin \phi$, showing that CD is greatest for a helix with a 45° pitch angle and is zero in the extreme limits of a helix that is compressed to a circle or stretched out to a straight rod. Again, this is consistent with the need for a chiral sample molecule. These factors also show that the CD signal is positive for right-handed helices (where $\phi > 0$) and negative for left-handed helices.

Assuming the validity of Ohm's law had the problems that we ignored both charge accumulation at the helix ends and the time required for an applied electric field to create a steady-state current. Handled correctly, these effects combine to enable electrical oscillations back and forth along the helix with a specific resonant frequency, as in an antenna. Unfortunately, Ohm's law does not apply in any regime; it is inaccurate for light frequencies above resonance because electric currents are not at steady-state, it is inaccurate below resonance because of charge accumulation at the helix ends, and it is inaccurate at resonance for both reasons. Thus, a better treatment of classical CD would account for resonance explicitly but is also substantially more complicated.

Quantum Explanation of CD

A quantum explanation for CD avoids the Ohm's law assumption and, obviously, accounts for quantum behaviors. Here, we expand upon the explanation given by Rodger and Nordén¹¹ to derive the Rosenfeld equation, on which most quantitative CD research is based.

A molecule's extinction coefficient can be found from Fermi's golden rule,¹⁷ which expresses transition probabilities between initial state $|i\rangle$ and final state $|f\rangle$, as

$$\epsilon = \frac{\pi N_A \omega \delta(\omega - \omega_{fi})}{\epsilon_0 \hbar c \ln 10} \frac{1}{E_0^2} |\langle f|H|i\rangle|^2 \quad (14)$$

where N_A is Avogadro's number, ϵ_0 is the electric permittivity of free space, \hbar is Planck's constant, $\delta(\omega - \omega_{fi})$ is a Dirac δ function, and H is the Hamiltonian operator for the interaction. The δ function has its peak where the photon energy equals the energy difference between the two states, making this the only frequency where the extinction coefficient is nonzero. When this condition is satisfied, the $|\langle f|H|i\rangle|^2$ term shows that the light absorption scales with the amount of coupling that the Hamiltonian creates between the initial and final states. For convenience, we subsume the first factor of eq 14 into the constant k .

The interaction Hamiltonian, which expresses the molecule energy in the light's electromagnetic field, is

$$H = -\boldsymbol{\mu} \cdot \mathbf{E} - \mathbf{m} \cdot \mathbf{B} + \text{higher order terms} \quad (15)$$

where $\boldsymbol{\mu}$ is the molecule's electric dipole moment, \mathbf{E} is the externally applied electric field, \mathbf{m} is the molecule's magnetic dipole moment, and \mathbf{B} is the externally applied magnetic field. We drop the higher order terms because they are not necessary for explaining CD. Although not immediately relevant, the electric and magnetic dipole moments for discrete particles enumerated with index i , each with charge q_i , mass m_i , location \mathbf{r}_i , and momentum \mathbf{p}_i are^{11,13}

$$\boldsymbol{\mu} = \sum_i q_i \mathbf{r}_i \quad (16)$$

$$\mathbf{m} = \frac{1}{2} \sum_i \frac{q_i}{m_i} \mathbf{r}_i \times \mathbf{p}_i \quad (17)$$

These equations come from classical physics but apply equally well in quantum mechanics upon replacement of the position and velocity vectors with their quantum operators.

Returning to eq 14, we expand the bracket and then substitute in the Hamiltonian:

$$\begin{aligned} \epsilon &= kE_0^{-2} \langle f|H|i\rangle^* \cdot \langle f|H|i\rangle \\ &= kE_0^{-2} \langle i|H|f\rangle \cdot \langle f|H|i\rangle \\ &= kE_0^{-2} \langle i|(-\boldsymbol{\mu} \cdot \mathbf{E} - \mathbf{m} \cdot \mathbf{B})|f\rangle \cdot \langle f|(-\boldsymbol{\mu} \cdot \mathbf{E} - \mathbf{m} \cdot \mathbf{B})|i\rangle \\ &= kE_0^{-2} [\langle i|(\boldsymbol{\mu} \cdot \mathbf{E})|f\rangle + \langle i|(\mathbf{m} \cdot \mathbf{B})|f\rangle] [\langle f|(\boldsymbol{\mu} \cdot \mathbf{E})|i\rangle \\ &\quad + \langle f|(\mathbf{m} \cdot \mathbf{B})|i\rangle] \end{aligned} \quad (18)$$

These \mathbf{E} - and \mathbf{B} -fields are real, but we would like to use complex fields, $\tilde{\mathbf{E}}$ and $\tilde{\mathbf{B}}$, so we can use the light polarization equations given previously. This substitution is allowable because the two terms in the equation are already complex conjugates of each other, a condition that needs to be maintained during the substitution, so the answer will necessarily be real at the end. This gives

$$\epsilon = kE_0^{-2} [\langle i|\boldsymbol{\mu}|f\rangle \cdot \tilde{\mathbf{E}}^* + \langle i|\mathbf{m}|f\rangle \cdot \tilde{\mathbf{B}}^*] [\langle f|\boldsymbol{\mu}|i\rangle \cdot \tilde{\mathbf{E}} + \langle f|\mathbf{m}|i\rangle \cdot \tilde{\mathbf{B}}] \quad (19)$$

Next, we substitute in for $\tilde{\mathbf{E}}$ and $\tilde{\mathbf{B}}$ from eqs 1 and 4. In the process, the magnitude of the electric field terms, E_0 , cancels out with the E_0^{-2} factor at the beginning of the equation. The

phase terms that get substituted into the first factor are $e^{-i(\mathbf{k}\mathbf{x} - \omega t)}$, and those that get substituted into the second factor are $e^{i(\mathbf{k}\mathbf{x} - \omega t)}$, so they multiply to 1 and drop out of the equation as well. Finally, we define the magnetic polarization vector for circularly polarized light, $\hat{\mathbf{b}}$, in terms of the electric polarization vector using eq 4 to give it as

$$\hat{\mathbf{b}} = \pm \frac{i}{c} \hat{\mathbf{e}} \quad (20)$$

Together, these simplify eq 19 to

$$\epsilon = k[\langle i|\boldsymbol{\mu}|f\rangle \cdot \hat{\mathbf{e}}^* + \langle i|\mathbf{m}|f\rangle \cdot \hat{\mathbf{b}}^*] [\langle f|\boldsymbol{\mu}|i\rangle \cdot \hat{\mathbf{e}} + \langle f|\mathbf{m}|i\rangle \cdot \hat{\mathbf{b}}] \quad (21)$$

To make sense of the brackets, we define the initial and final state bras and kets as

$$\langle i| = [1 \ 0] \quad \langle f| = [0 \ 1] \quad |i\rangle = \begin{bmatrix} 1 \\ 0 \end{bmatrix} \quad |f\rangle = \begin{bmatrix} 0 \\ 1 \end{bmatrix} \quad (22)$$

The electric and magnetic dipole moment operators can then be written as

$$\boldsymbol{\mu} = \begin{bmatrix} \boldsymbol{\mu}_{ii} & \boldsymbol{\mu}_{fi} \\ \boldsymbol{\mu}_{if} & \boldsymbol{\mu}_{ff} \end{bmatrix} \quad \mathbf{m} = \begin{bmatrix} \mathbf{m}_{ii} & \mathbf{m}_{fi} \\ \mathbf{m}_{if} & \mathbf{m}_{ff} \end{bmatrix} \quad (23)$$

where each matrix element represents a bracket. In the electric dipole matrix, $\boldsymbol{\mu}_{ii} = \langle i|\boldsymbol{\mu}|i\rangle$, which is the static electric dipole moment of the molecule in its initial state, and $\boldsymbol{\mu}_{ff} = \langle f|\boldsymbol{\mu}|f\rangle$, which is the static electric dipole moment of the molecule in its final state. The off-diagonal elements, $\boldsymbol{\mu}_{fi}$ and $\boldsymbol{\mu}_{if}$ are the electric transition dipole moments, which enable coupling between the states by electric fields. By convention, the subscript order is reversed from the bracket order, so that $\boldsymbol{\mu}_{fi} = \langle i|\boldsymbol{\mu}|f\rangle$ and vice versa.¹¹ The $\boldsymbol{\mu}$ matrix is Hermitian, so $\boldsymbol{\mu}_{fi} = \boldsymbol{\mu}_{if}^*$. Although not obvious here, it is possible to choose the $|i\rangle$ and $|f\rangle$ wave functions so that $\boldsymbol{\mu}_{fi}$ is real, in which case $\boldsymbol{\mu}_{fi} = \boldsymbol{\mu}_{if}$. The magnetic dipole matrix is analogous, giving the static magnetic dipole moments in the initial and final states on the diagonal and the magnetic transition dipole moments in the off-diagonal terms. However, wave functions that make $\boldsymbol{\mu}_{fi}$ real necessarily make \mathbf{m}_{fi} imaginary (this arises from the momentum factor in eq 17, for which the quantum operator is $-i\hbar \partial/\partial x$), implying that $\mathbf{m}_{fi} = -\mathbf{m}_{if}$.

These dipole moment definitions simplify the extinction coefficient to

$$\begin{aligned} \epsilon &= k[\boldsymbol{\mu}_{fi} \cdot \hat{\mathbf{e}}^* + \mathbf{m}_{fi} \cdot \hat{\mathbf{b}}^*] [\boldsymbol{\mu}_{if} \cdot \hat{\mathbf{e}} + \mathbf{m}_{if} \cdot \hat{\mathbf{b}}] \\ &= k[(\boldsymbol{\mu}_{fi} \cdot \hat{\mathbf{e}}^*)(\boldsymbol{\mu}_{if} \cdot \hat{\mathbf{e}}) + (\mathbf{m}_{fi} \cdot \hat{\mathbf{b}}^*)(\mathbf{m}_{if} \cdot \hat{\mathbf{b}}) + (\boldsymbol{\mu}_{fi} \cdot \hat{\mathbf{e}}^*)(\mathbf{m}_{if} \cdot \hat{\mathbf{b}}) \\ &\quad + (\mathbf{m}_{fi} \cdot \hat{\mathbf{b}}^*)(\boldsymbol{\mu}_{if} \cdot \hat{\mathbf{e}})] \end{aligned} \quad (24)$$

As with the classical version of this in eq 11, the first term represents absorption of light due to its electric field, the second term represents absorption due to its magnetic field, and the last two terms are cross-terms that represent interactions from both the electric and magnetic fields. These latter terms produce circular dichroism.

The CD extinction coefficient is the difference between the LCP and RCP extinction coefficients, $\epsilon_{CD} = \epsilon_L - \epsilon_R$, which is

$$\begin{aligned}\epsilon_{\text{CD}} = & k\{[(\boldsymbol{\mu}_{fi} \cdot \hat{\mathbf{e}}_L^*)(\boldsymbol{m}_{if} \cdot \hat{\mathbf{e}}_L) - (\boldsymbol{\mu}_{fi} \cdot \hat{\mathbf{e}}_R^*)(\boldsymbol{m}_{if} \cdot \hat{\mathbf{e}}_R)] \\ & + [(\boldsymbol{m}_{fi} \cdot \hat{\mathbf{b}}_L^*)(\boldsymbol{m}_{if} \cdot \hat{\mathbf{b}}_L) - (\boldsymbol{m}_{fi} \cdot \hat{\mathbf{b}}_R^*)(\boldsymbol{m}_{if} \cdot \hat{\mathbf{b}}_R)] \\ & + [(\boldsymbol{\mu}_{if} \cdot \hat{\mathbf{e}}_L)(\boldsymbol{m}_{fi} \cdot \hat{\mathbf{b}}_L^*) - (\boldsymbol{\mu}_{if} \cdot \hat{\mathbf{e}}_R)(\boldsymbol{m}_{fi} \cdot \hat{\mathbf{b}}_R^*)] \\ & + [(\boldsymbol{\mu}_{fi} \cdot \hat{\mathbf{e}}_L^*)(\boldsymbol{m}_{if} \cdot \hat{\mathbf{b}}_L) - (\boldsymbol{\mu}_{fi} \cdot \hat{\mathbf{e}}_R^*)(\boldsymbol{m}_{if} \cdot \hat{\mathbf{b}}_R)]\}\end{aligned}$$

where $\hat{\mathbf{e}}_L$, $\hat{\mathbf{e}}_R$, $\hat{\mathbf{b}}_L$, and $\hat{\mathbf{b}}_R$ are the electric and magnetic polarization vectors for LCP and RCP. In terms of the left and right unit vectors, the electric polarization vectors are $\hat{\mathbf{e}}_L = \hat{\mathbf{1}}$ and $\hat{\mathbf{e}}_R = \hat{\mathbf{r}}$ (from eqs 2 and 3), and the magnetic polarization vectors are $\hat{\mathbf{b}}_L = -\hat{\mathbf{i}}/c$ and $\hat{\mathbf{b}}_R = -\hat{\mathbf{i}}/c$ (from eq 20). Substituting and simplifying gives

$$\begin{aligned}\epsilon_{\text{CD}} = & k\{[(\boldsymbol{\mu}_{fi} \cdot \hat{\mathbf{r}})(\boldsymbol{m}_{if} \cdot \hat{\mathbf{1}}) - (\boldsymbol{\mu}_{fi} \cdot \hat{\mathbf{1}})(\boldsymbol{m}_{if} \cdot \hat{\mathbf{r}})] \\ & + c^{-2}[(\boldsymbol{m}_{fi} \cdot \hat{\mathbf{r}})(\boldsymbol{m}_{if} \cdot \hat{\mathbf{1}}) - (\boldsymbol{m}_{fi} \cdot \hat{\mathbf{1}})(\boldsymbol{m}_{if} \cdot \hat{\mathbf{r}})] \\ & + ic^{-1}[(\boldsymbol{\mu}_{if} \cdot \hat{\mathbf{1}})(\boldsymbol{m}_{fi} \cdot \hat{\mathbf{r}}) + (\boldsymbol{\mu}_{if} \cdot \hat{\mathbf{r}})(\boldsymbol{m}_{fi} \cdot \hat{\mathbf{1}})] \\ & + ic^{-1}[-(\boldsymbol{\mu}_{fi} \cdot \hat{\mathbf{r}})(\boldsymbol{m}_{if} \cdot \hat{\mathbf{1}}) - (\boldsymbol{\mu}_{fi} \cdot \hat{\mathbf{1}})(\boldsymbol{m}_{if} \cdot \hat{\mathbf{r}})]\}\end{aligned}$$

Next, we use the statements given earlier that $\boldsymbol{\mu}_{fi} = \boldsymbol{\mu}_{if}$ and $\boldsymbol{m}_{fi} = -\boldsymbol{m}_{if}$ to find that the first two terms are each equal to zero and the last two terms are equal to each other. These simplify the CD extinction coefficient to

$$\epsilon_{\text{CD}} = -\frac{2ik}{c}[(\boldsymbol{\mu}_{fi} \cdot \hat{\mathbf{r}})(\boldsymbol{m}_{if} \cdot \hat{\mathbf{1}}) + (\boldsymbol{\mu}_{fi} \cdot \hat{\mathbf{1}})(\boldsymbol{m}_{if} \cdot \hat{\mathbf{r}})] \quad (25)$$

Finally, we need to think about three-dimensional space. The electric transition dipole moment $\boldsymbol{\mu}_{fi}$ is a vector, which we write as $[\mu_{fi}^X, \mu_{fi}^Y, \mu_{fi}^Z]$, and \boldsymbol{m}_{if} is the vector $[m_{if}^X, m_{if}^Y, m_{if}^Z]$. The uppercase X, Y, and Z indices show that they are expressed in the laboratory coordinate system. Taking the dot product of these vectors with $\hat{\mathbf{1}}$, from eq 3, leads to

$$\begin{aligned}\boldsymbol{\mu}_{fi} \cdot \hat{\mathbf{1}} &= \frac{1}{\sqrt{2}}(\mu_{fi}^Y + i\mu_{fi}^Z) \\ \boldsymbol{m}_{if} \cdot \hat{\mathbf{1}} &= \frac{1}{\sqrt{2}}(m_{if}^Y + im_{if}^Z)\end{aligned}$$

The dot products with $\hat{\mathbf{r}}$ are the same but have negative second terms. Substituting these results into eq 25, expanding the binomials, and simplifying gives

$$\epsilon_{\text{CD}} = -\frac{2ik}{c}(\mu_{fi}^Y m_{if}^Y + \mu_{fi}^Z m_{if}^Z)$$

Both sides of this equation are real. On the right side, the μ_{fi} values are real, and the m_{if} values are imaginary, and then multiplication by i in the prefactor makes the value real again. Nevertheless, we take the real part of the right side anyhow, which then simplifies to

$$\epsilon_{\text{CD}} = \frac{2k}{c}\text{Im}(\mu_{fi}^Y m_{if}^Y + \mu_{fi}^Z m_{if}^Z) \quad (26)$$

This is the CD extinction coefficient for a single molecule, or a population of molecules that all have the same orientation. As in the classical treatment, the CD signal arises from a product of electric and magnetic factors. The electric and magnetic dipole moments that ended up in this final equation are the ones that are along the y - and z -axes, arising from the fact that the light's \mathbf{E} - and \mathbf{B} -fields are also along these axes.

Rotational Averaging

To convert the CD result calculated above, eq 26, so that it applies to unoriented molecules, we follow the rotational averaging procedure described by Andrews.¹⁸ The μ_{fi}^Y value is the dot product of the transition dipole moment vector in the lab frame with the lab frame's unit y vector, $\mu_{fi}^Y = \boldsymbol{\mu}_{fi}^L \cdot \hat{\mathbf{y}}$, where the superscript L indicates the lab frame. Writing the transition dipole moment in the molecule frame as $\boldsymbol{\mu}_{fi}$, we rotate from the molecule frame to the lab frame by right-multiplying by the direction cosine matrix $\boldsymbol{\Phi}$, which depends on the molecule's rotation angles, giving $\boldsymbol{\mu}_{fi}^L = \boldsymbol{\mu}_{fi} \boldsymbol{\Phi}$. These substitutions, and comparable ones for the magnetic transition dipoles and z -axis components, expand eq 26 to

$$\epsilon_{\text{CD}} = \frac{2k}{c}\text{Im}[(\boldsymbol{\mu}_{fi} \boldsymbol{\Phi} \hat{\mathbf{y}})(\boldsymbol{m}_{if} \boldsymbol{\Phi} \hat{\mathbf{y}}) + (\boldsymbol{\mu}_{fi} \boldsymbol{\Phi} \hat{\mathbf{z}})(\boldsymbol{m}_{if} \boldsymbol{\Phi} \hat{\mathbf{z}})] \quad (27)$$

Integrating over all possible molecule orientations, denoted with angle brackets, gives rotationally averaged values. The first term expands to

$$\begin{aligned}\langle (\boldsymbol{\mu}_{fi} \boldsymbol{\Phi} \hat{\mathbf{y}})(\boldsymbol{m}_{if} \boldsymbol{\Phi} \hat{\mathbf{y}}) \rangle &= \langle (\mu_{fi}^X \Phi_{Yx} + \mu_{fi}^Y \Phi_{Yy} + \mu_{fi}^Z \Phi_{Yz})(m_{if}^X \Phi_{Yx} + m_{if}^Y \Phi_{Yy} + m_{if}^Z \Phi_{Yz}) \rangle \\ &= \left\langle \left(\sum_j \mu_{fi}^j \Phi_{Yj} \right) \left(\sum_k m_{if}^k \Phi_{Yk} \right) \right\rangle = \sum_{j,k} \mu_{fi}^j m_{if}^k \langle \Phi_{Yj} \Phi_{Yk} \rangle\end{aligned}$$

Lowercase superscripts represent the molecule's reference frame. The angle brackets compressed down to only include the direction cosine matrix terms in the last equality because those are the only factors that depend on the molecule's rotation angle. These terms integrate¹⁸ to zero if $j \neq k$ and $1/3$ if $j = k$, which simplifies the rotational average to

$$\langle (\boldsymbol{\mu}_{fi} \boldsymbol{\Phi} \hat{\mathbf{y}})(\boldsymbol{m}_{if} \boldsymbol{\Phi} \hat{\mathbf{y}}) \rangle = \sum_{j,k} \mu_{fi}^j m_{if}^k \frac{\delta_{j,k}}{3} = \frac{1}{3} \boldsymbol{\mu}_{fi} \cdot \boldsymbol{m}_{if} \quad (28)$$

The $\delta_{j,k}$ factor is a Kronecker δ function. The second term of eq 27 is analogous and has the same result.

Substituting these results into eq 27 gives the CD for randomly oriented molecules as

$$\epsilon_{\text{CD}} = \frac{4k}{3c}\text{Im}(\boldsymbol{\mu}_{fi} \cdot \boldsymbol{m}_{if}) \quad (29)$$

This, or versions with slightly different constants in the initial factor, is called the Rosenfeld equation.^{8,11}

CD of a Quantum Harmonic Oscillator

We illustrate the use of the Rosenfeld equation, eq 29, by calculating the CD for a sample of unoriented one-dimensional harmonic oscillators,^{17,19} each of which lies along the path of a three-dimensional helix.²⁰ For each, we assume that an electron, with charge e and mass m_e is elastically bound to the helix midpoint by a spring with force constant k_e and that its range of travel extends over multiple helix turns.

The eigenstates for the oscillator are the kets $|n\rangle$, where $n = 0, 1, 2, \dots$. Their energy levels are^{17,19}

$$E_n = \hbar\omega_e \left(n + \frac{1}{2} \right) \quad (30)$$

where ω_e is the oscillator frequency, equal to $\sqrt{k_e/m_e}$. We consider the absorption of light as the electron is excited from $|n\rangle$ to $|n+1\rangle$. The electric dipole moment is $\boldsymbol{\mu} = e\mathbf{r}$ (eq 16).

Defining the molecule's z -axis as parallel to the helix axis, as usual, the x - and y -components of μ are equal to zero due to our assumption that the electron's range extends over multiple helix turns, implying that $\mu^z = ez$. In terms of the path length along the helix, the electric dipole moment is

$$\mu^z = es \cos \phi \quad (31)$$

For excitation from $|n\rangle$ to $|n+1\rangle$, the electric transition dipole along z is

$$\begin{aligned} \mu_{fi}^z &= \langle n | \mu^z | n+1 \rangle \\ &= e \cos \phi \langle n | s | n+1 \rangle \\ &= e \cos \phi \sqrt{\frac{\hbar(n+1)}{2m_e\omega_e}} \end{aligned} \quad (32)$$

where the final equality is a standard result, often found with raising and lowering operators.^{17,19} The magnetic moment is $\mathbf{m} = e\mathbf{r} \times \mathbf{p}/2m_e$ from eq 17, of which only the z -component is nonzero again, giving

$$m^z = \frac{er}{2m_e} p_s \sin \phi \quad (33)$$

where r is the helix radius, as usual, and p_s is the electron momentum along the helix path. The magnetic transition dipole along z for the transition is

$$\begin{aligned} m_{fi}^z &= \langle n+1 | m^z | n \rangle \\ &= \frac{er}{2m_e} \sin \phi \langle n+1 | p_s | n \rangle \\ &= \frac{ier}{2m_e} \sin \phi \sqrt{\frac{m_e \hbar \omega_e (n+1)}{2}} \end{aligned} \quad (34)$$

Again, the final equation is a standard result.^{17,19}

Substituting the transition dipole moments into the Rosenfeld equation gives the CD extinction coefficient

$$\begin{aligned} \epsilon_{\text{CD}} &= \frac{4k}{3c} \text{Im} \left(\frac{ie^2 \hbar r (n+1)}{4m_e} \cos \phi \sin \phi \right) \\ &= \frac{ke^2 \hbar r (n+1)}{3m_e c} \cos \phi \sin \phi \end{aligned}$$

We expand the constants that got subsumed into k earlier to give the result

$$\epsilon_{\text{CD}} = \frac{\pi N_A \omega_e^2 r (n+1) \delta(\omega - \omega_e)}{3\epsilon_0 m_e c^2 \ln 10} \cos \phi \sin \phi \quad (35)$$

Comparison with the classical calculation of the CD power dissipation for a conducting helix (eq 13) shows good agreement. Both are proportional to r and ω from the \mathbf{B} -field influence, to $\cos \phi$ from the projection of the \mathbf{E} -field onto the helix path, and to $\sin \phi$ from the projection of the \mathbf{B} -field onto a perpendicular to the helix path. Also, both results predict a positive CD signal for right-handed helices and a negative signal for left-handed helices.

Numerical Prediction of Protein Circular Dichroism

Finally, we use these results to estimate the far-ultraviolet CD effect for a protein α -helix, which can then be compared against experiment (blue line in Figure 5). This absorption

band arises from amide transitions along the backbone of the polypeptide chain²¹ and has been analyzed extensively.

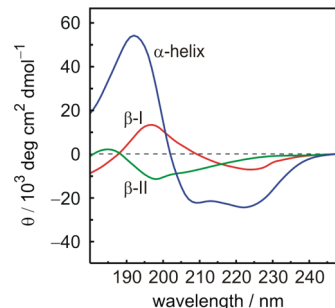


Figure 5. CD spectra for protein secondary structures: α -helix in blue, β -sheet (β_I) in red, and disordered proteins and left-handed polyproline II helices (β_{II}) in green. Reprinted with permission from ref 22. Copyright 2007 Royal Society of Chemistry.

Here, we interpret this transition using the harmonic oscillator model just derived, which is a crude approximation for this system but still instructive. An α -helix has a radius of about 0.23 nm and a pitch of about 0.54 nm, where the pitch is the helix rise over one full turn.²³ From the unrolled helix shown in Figure 4, $\tan \phi = 2\pi r/p$ where p is the pitch, giving the α -helix pitch angle as $\phi = 69.5^\circ$. From Figure 5, the wavelength for the center of the CD peak is around 190 nm, which corresponds to a frequency of $\omega = 9.9 \times 10^{15} \text{ s}^{-1}$. Substituting these values into eq 35, along with the fundamental constants $e = 1.602 \times 10^{-19} \text{ C}$, $\epsilon_0 = 8.854 \times 10^{-12} \text{ C}^2 \text{ kg}^{-1} \text{ m}^{-3} \text{ s}^2$, $m_e = 9.109 \times 10^{-31} \text{ kg}$, $c = 3.00 \times 10^8 \text{ m/s}$, and $N_A = 6.022 \times 10^{23} \text{ mol}^{-1}$, gives the result

$$\epsilon_{\text{CD}} = (7.2 \times 10^{15} \text{ m}^2 \text{ mol}^{-1} \text{ s}^{-1})(n+1)\delta(\omega - \omega_e) \quad (36)$$

We assume excitation from the ground state of the harmonic oscillator, meaning that $n = 0$. Also, we integrate over the absorption band so that the Dirac δ function integrates to 1. Doing so leads to our prediction for the peak area of the CD extinction coefficient spectrum

$$\int \epsilon_{\text{CD}} d\omega = 7.2 \times 10^{15} \text{ m}^2 \text{ mol}^{-1} \text{ s}^{-1} \quad (37)$$

Some unit conversion is required to compare this prediction with the results shown in Figure 5. First of all, the figure's y -axis is measured in degrees, implying that the CD effect is reported in units of ellipticity. These convert to extinction coefficient units according to¹¹

$$\epsilon_{\text{CD}} = \epsilon_l - \epsilon_r = \frac{4\pi\theta}{180 \ln 10} = \frac{\theta}{32.982} \quad (38)$$

Additionally, the $\text{cm}^2 \text{ dmol}^{-1}$ units on the y -axis convert to SI units with $1 \text{ cm}^2 \text{ dmol}^{-1} = 10^{-3} \text{ m}^2 \text{ mol}^{-1}$. Using this, the peak height of the blue curve is about $55 \times 10^3 \text{ deg cm}^2 \text{ dmol}^{-1}$, which converts to $\Delta\epsilon = 1.67 \text{ m}^2 \text{ mol}^{-1}$. On the x -axis, the α -helix peak extends from about 180 to 200 nm, which corresponds to a width of $\Delta\omega = 1.05 \times 10^{15} \text{ s}^{-1}$. The product of peak height and width gives a rough estimate of the peak area, which is

$$\int \epsilon_{\text{CD}} d\omega \approx 1.8 \times 10^{15} \text{ m}^2 \text{ mol}^{-1} \text{ s}^{-1} \quad (39)$$

This is a factor of 4 smaller than the prediction made above, including having the same sign, which is remarkably close given

the substantial approximations that were made in applying a harmonic oscillator model to the molecular orbital transitions in the protein backbone. Even if the good agreement is partly coincidence, this result at least shows that the harmonic oscillator model calculation is likely to yield predictions with the correct general magnitude.

CONCLUSION

This work presents several theoretical results on circular dichroism. It presents a classical explanation that shows how electron oscillations in a helical molecule interact with both the electric and magnetic fields of a light wave to yield different absorptions for left and right circularly polarized light (eq 13). This result is straightforward and conceptually correct in many ways but not quantitative due to its application of Ohm's law to a non-steady-state system. A quantum explanation (eqs 27 and 30) is less intuitive but more accurate, and it forms the basis of most current CD research. We applied it to a one-dimensional harmonic oscillator that is confined to a three-dimensional helix, leading to a result (eq 35) that has strong similarities to the classical CD case. It also applies surprisingly well to the CD effect for protein α -helices, predicting a CD effect that is about a factor of 4 larger than the experimental result.

AUTHOR INFORMATION

Corresponding Author

Steven S. Andrews – Department of Physics, Seattle University, Seattle, Washington 98122, United States;
orcid.org/0000-0002-4576-8107; Email: andrewss@seattleu.edu

Author

James Tretton – Department of Physics, Seattle University, Seattle, Washington 98122, United States

Complete contact information is available at:

<https://pubs.acs.org/10.1021/acs.jchemeduc.0c01061>

Notes

The authors declare no competing financial interest.

ACKNOWLEDGMENTS

This work was initiated as J.T.'s mathematics senior synthesis project, overseen by Dylan Helliwell, who provided valuable feedback.

REFERENCES

- (1) Johnson, W. C., Jr Secondary structure of proteins through circular dichroism spectroscopy. *Annu. Rev. Biophys. Biophys. Chem.* **1988**, *17*, 145–166.
- (2) Kelly, S. M.; Jess, T. J.; Price, N. C. How to study proteins by circular dichroism. *Biochim. Biophys. Acta, Proteins Proteomics* **2005**, *1751*, 119–139.
- (3) Greenfield, N. J. Using circular dichroism spectra to estimate protein secondary structure. *Nat. Protoc.* **2006**, *1*, 2876.
- (4) Stephens, P. J. Theory of vibrational circular dichroism. *J. Phys. Chem.* **1985**, *89*, 748–752.
- (5) Stephens, P.; Lowe, M. Vibrational circular dichroism. *Annu. Rev. Phys. Chem.* **1985**, *36*, 213–241.
- (6) Freedman, T. B.; Cao, X.; Dukor, R. K.; Nafie, L. A. Absolute configuration determination of chiral molecules in the solution state using vibrational circular dichroism. *Chirality* **2003**, *15*, 743–758.

(7) Cotton, M. Recherches sur l'absorption et la dispersion de la lumière par les milieux doués du pouvoir rotatoire. *J. Phys. Theor. Appl.* **1896**, *5*, 237–244.

(8) Rosenfeld, L. Quantenmechanische Theorie der natürlichen optischen Aktivität von Flüssigkeiten und Gasen. *Eur. Phys. J. A* **1929**, *52*, 161–174.

(9) Atkins, P.; Woolley, R. On the theory of optical activity. *Proc. R. Soc. London A Math. Phys. Sci.* **1970**, *314*, 251–267.

(10) Schellman, J. A. Circular dichroism and optical rotation. *Chem. Rev.* **1975**, *75*, 323–331.

(11) Rodger, A.; Nordén, B. *Circular Dichroism and Linear Dichroism*; Oxford University Press: Oxford, 1997.

(12) Kobayashi, N.; Muranaka, A.; Mack, J. *Circular Dichroism and Magnetic Circular Dichroism Spectroscopy for Organic Chemists*; Royal Society of Chemistry: Cambridge, UK, 2011.

(13) Griffiths, D. J. *Introduction to Electrodynamics*, 2nd ed.; Prentice Hall: Englewood Cliffs, NJ, 1989.

(14) Bublitz, G. U.; Boxer, S. G. Stark spectroscopy: applications in chemistry, biology, and materials science. *Annu. Rev. Phys. Chem.* **1997**, *48*, 213–242.

(15) Andrews, S. S.; Boxer, S. G. Vibrational Stark effects of nitriles II. Physical origins of stark effects from experiment and perturbation models. *J. Phys. Chem. A* **2002**, *106*, 469–477.

(16) Hecht, E. *Optics*; Pearson: San Francisco, 2015.

(17) Sakurai, J. J.; Tuan, S. F. *Modern Quantum Mechanics, Revised Edition*; Addison-Wesley: Reading, MA, 1994.

(18) Andrews, S. S. Using rotational averaging to calculate the bulk response of isotropic and anisotropic samples from molecular parameters. *J. Chem. Educ.* **2004**, *81*, 877.

(19) Cohen-Tannoudji, C.; Diu, B.; Laloë, F. *Quantum Mechanics*; Wiley Interscience: New York, 1977.

(20) Tinoco, I., Jr; Woody, R. W. Optical rotation of oriented helices. IV. A free electron on a helix. *J. Chem. Phys.* **1964**, *40*, 160–165.

(21) Sreerama, N.; Woody, R. W. Computation and analysis of protein circular dichroism spectra. *Methods Enzymol.* **2004**, *383*, 318–351.

(22) Bulheller, B. M.; Rodger, A.; Hirst, J. D. Circular and linear dichroism of proteins. *Phys. Chem. Chem. Phys.* **2007**, *9*, 2020–2035.

(23) Schulz, G. E.; Schirmer, R. H. *Principles of Protein Structure*; Springer: New York, 1979.